

IRAQI

Academic Scientific Journals

Alkadhum Journal of Science (AKJS)

Journal Homepage: <https://alkadhum-col.edu.iq/JKCEAS>

A Statistical Analysis of COVID-19 Image Detection Using the Wavelet Transform

¹Hadi R. Ali and ²Falah A. Bida

¹ Imam Al-Kadhum College, Department of Computer Techniques Engineering, Baghdad, Iraq.

² Directorate of Education in Baghdad / Rusafa III, Ministry of Education, Baghdad, Iraq.

Article information

Article history:

Received: October, 19, 2023

Accepted: November, 20, 2023

Available online: December, 14, 2023

Keywords:

Covid-19 detection,
Magnetism Resonant Imaging (MRI),
Calculated Tomography (CT),
Discrete Wavelet Transform (DWT),
Fusing

*Corresponding Author:

Full Name

diddiddodo19@gmail.com

DOI:

<https://doi.org/10.61710/akjs.v1i2.49>

This article is licensed under:

[Creative Commons Attribution 4.0 International License](https://creativecommons.org/licenses/by/4.0/).

Abstract

Since December 2019, the world has been struggling Against the discovered virus called Covid-19, which Its symptoms are similar to pneumonia. Being highly contagious, it is It spread all over the world, hence the World Health Organization By declaring this disease as a global pandemic. some Patients infected with this virus suffer from severe symptoms And deadly. Hence the importance of early detection of Coronavirus (COVID-19). COVID-19 is a disease that affects the respiratory system of the human body, and detecting this disease is complex and one of the main challenges. This work proposed a technique to detect COVID-19 by integrating multifocal images based on wavelet transduction. So, to achieve the detection of COVID-19, Magnet resonant imagery (MRI) and computation tomography (CT) have been used. The multifocal image was included to support the diagnosis made by the clinicians. The seven wave-based algorithms bior2.2, coif2, db2, dmey, rbio2.2, sym4, and haar, respectively, were used to achieve a range of results. This approach effectively combines the data obtained from CT and MRI scans to produce a merged image that improves disease diagnosis efficiency by using MATLAB to determine the efficiency of the algorithm. The signal-to-noise ratio (PSNR) and the entropy factor are used to measure the image fusion efficiency. The statistical analysis of the final images demonstrated the superiority of the image attributes over both the CT image and the MRI.

1. Introduction

The virus that causes severe acute respiratory syndrome (Coronavirus), which has been labeled and the Health Organization has declared a worldwide problem, is known as COVID-19. Soft tissue information is provided by magnetic resonance imaging (MRI), while bone features are revealed by computed tomography (CT). Image fusion is a method of combining a large chrominance image with limited spectral information to produce the highest multitemporal image that contains both multispectral image with large location data and color information [1].

This method is used to optimize image data and enhance image quality. It is highly beneficial to detect disorders and associated diagnoses such that appropriate treatment can be given. Previous studies focused on detecting COVID-19 using different techniques such as random vector functional link (RVFL) network [2], transfer learning [3], Deeper sound encoders and wavelet scattering features retrieved from limited image features [4], Discrete wavelet transform (DWT) and empirical mode decomposition (EMD)[5], and a support vector machine (SVM) classifier and DWT [6].

2. Fundamental Concepts

2.1. Transform of Wavelets

Wavelet transformations are used to break down a signal into levels, each of which corresponds to a lower focal wave and greater frequency ranges and resolution. Continuous and discrete conversions are the two basic types of conversions. DWT, which continuously adds 2-channel filter banks on the lower range with downsampling (initially the original signal). The wavelet form is thus the Minimal of wavelet-based CT and MRI image integration which convert two low-resolution pass bands and the increased bands produced at every step into two high-resolution passage band. This transformation is non-redundant and invertible. The DWT is a space-time reduction that can be used to analyze multi-resolution images. The DWT's primary principle describes signals as a combination of wavelets. The wavelet decomposition is [7]:

$$f(t) = \sum_{m,n} c_{m,n} \psi_{m,n}(t) \quad (1)$$

Where $f(t)$ is a discrete signal, $\psi_{m,n}(t) = 2^{-\frac{m}{2}} \psi[2^{-m}t - n]$ and m and n are integers. There are highly specific values of ψ like that $\psi_{m,n}(t)$ is an axial foundation, allowing parameters of the wavelet decomposition to be calculated internally:

$$c_{m,n} = (f, \psi_{m,n}) = \int \psi_{m,n}(t) f(t) dt \quad (2)$$

A scaling function $\phi_{m,n}$, as well as its dilated and translated form, are required to build a multiresolution analysis described in eq. (3):

$$\phi_{m,n}(t) = 2^{-\frac{m}{2}} \phi[2^{-m}t - n] \quad (3)$$

Depending on the characteristics of the covered level space and by expanding it into the appropriate areas, the $f(t)$ can be decomposed into finer components and features of varied sizes. As a result, extra coefficients $a_{m,n}$ are necessary at each scale to obtain such decomposition directly. At every level, the coefficients $a_{m,n}$ and $a_{m-1,n}$ define the estimates of the functional $f(t)$ for resolutions of 2^m and 2^{m-1} , respectively, whereas the coefficient $c_{m,n}$ and (missing thing) reflect the information loss when switching between approximations. To get $a_{m,n}$ at each level and location, it is possible to extract the wavelet and approximation coefficients as [7]:

$$a_{m,n} = \sum_k h_k 2^{(2-k)} a_{m-1,k} \quad (4)$$

$$c_{m,n} = \sum_k g_k 2^{(2-k)} a_{m-1,k} \quad (5)$$

Where g_n , h_n are higher and lower passing FIR filter that is linked to h_n . The analytical filter could be chosen from one biological package that has a corresponding set of synthesized filters \tilde{h} and \tilde{g} in order to rebuild the original signals. The signal is excellently reconstructed using these synthesis filters:

$$a_{m-1,l}(f) = \sum_n [\tilde{h}_k 2^{(2-l)} a_{m-n}(f) + \tilde{g}_k 2^{(2-l)} a_{m-n}(f)] \quad (6)$$

Filtering and down sampling are used to perform eqs. (4-6), on the other hand, is initial up sampling and filtering.

2.2. Image Fusing using Wavelet Transform

In DWT, the original images of source and target images are decomposed. This is demonstrated by the representation of many states, each of which represents a distinct parameter (horizontal, vertical, diagonal, and zero). The various black squares related to each level of decomposition are associated with the coefficient of the identical spatial structure of the image in each original image, which has the same pixel coordinates in the original

image. Inverse discrete wavelet transform (IDWT) creates the final fused image after obtaining a fused multi-scale [8] as shown in figure (1).

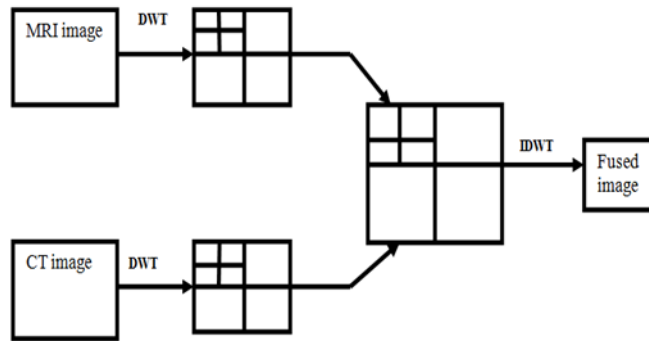


Figure 1. Image fusion of MRI and CT using wavelet decomposition.

Wavelet transformation fusion is a type of image fusion that is used to modify images. It incorporates all methods for merging in the field of conversion, transforming images according to specific merging criteria before returning to the waveform. As a result, the wavelet transformation fusion was more explicitly established by examining the collected MRI $I_1(x, y)$ and CT $I_2(x, y)$ images. After calculating the reversed wavelet translation, the combined image $I(x, y)$ is reconstructed [7]:

$$I(x, y) = \omega^{-1} \left(\varphi \left(\omega(I_1(x, y)), \omega(I_2(x, y)) \right) \right) \quad (7)$$

2.3. Wavelet Analysis

Wavelet analysis can be useful for discovering data properties such as trends, pauses, higher derived break, and identity that are missed by conventional signal analysis approaches. Wavelet analysis reduces or removes noise from the signal without inflicting real damage. Wavelet analysis is therefore essential when dealing with critical information, such as medical imaging [9]. The fundamental algorithm separates the input CT and images MRI into images of secondary decay breakdown at the second level, as shown in figure (2).

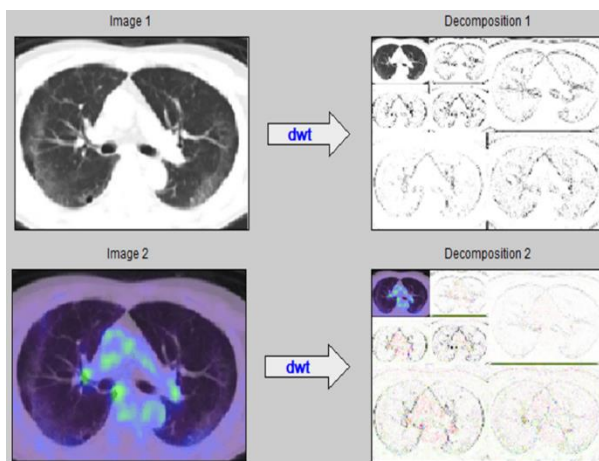


Figure 2. Wavelet decomposition on two levels of CT and MRI image

To approximate the CT and MRI images, at every level, low-pass (L) and high-pass (H) filtration are used to deconstruct them into rows and columns. Low-Low (LL) and Low-High (LH), High-Low (HL), and High-High

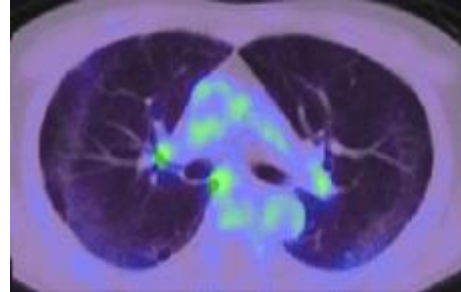
(HH) coefficients are described in depth. Smooth filters or low-pass filters are related to the scaling function, while high-pass filtering is associated with the wavelet function [10].

3. Samples Images and Algorithm

Below, in figure (3), sample images and proposed scheme of Algorithm in figure (4).



Lung CT Scan png 208 * 142



Lung MRI Scan png 228 * 133

Figure (3). Images samples

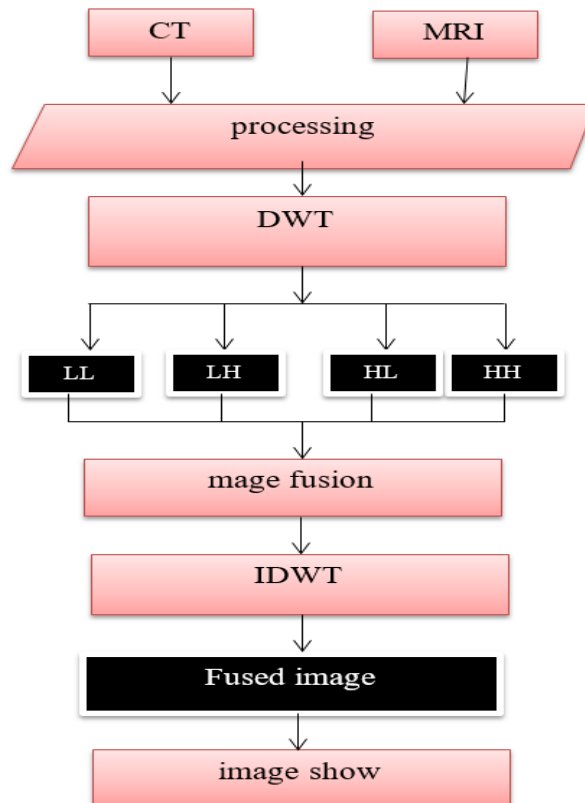


Figure 4. shows the algorithm's flow chart.

4. The Proposed Work

In the current study, the infected image data obtained by MRI and CT were inserted as a matrix of pixels in two dimensions of the matrix using MATLAB R2016. Images are shown in grayscale or different brightness, and data is saved in MATLAB. Normally, these images can be described by providing a big matrix with entrance points ranging from 0 to 255. This method involves multiple steps.

1- First step:

The source images (MRI and CT scans) of the sample are processed in this step to improve the contrast and brightness before being downsized to 128 * 128.

2- Second step:

The MRI and CT images are subjected to wavelet transformation, and for the best outcomes, they are mixed individually using various wavelet filters (Coiflets, Daubechies, haar, etc.).

3- Third step:

By integrating MRI and CT, wavelet approaches are applied to get the best results possible utilizing the currently available methodologies. These techniques utilize the total optimum of the wavelet coefficients with increased brightness while keeping the salient qualities in each image.

4- Fourth step:

By applying the proper threshold values to acquire the best result, the merged images are transformed into a binary format for easy calculation and greater detection effectiveness. According to the suggestion algorithm, the image is read as a 2D matrix consisting of 1 and 0, where 1 represents the white color and 0 represents the black color. By comparing each pixel with the corresponding pixel in the binary image, the infection can be detected with low error.

5- Fifth step:

After performing the inverse wavelet transform the reconstructed image is obtained. The performance of a reconstructed image is assessed using the statistics Peak Signal to Noise Ratio (PSNR) and Entropy Factor, which vary for the first and second stages of wavelet decomposition. The PSNR is described by [10]:

$$\text{PSNR} = 20 * \log \left(\frac{256}{\text{MSE}} \right) \quad (8)$$

Where MSE is the root mean square error which is calculated using the formula below:

$$\text{MSE} = \left[\sum_i (r_i - d)^2 \right]^{\frac{1}{2}} \quad (9)$$

Where r, and d are the origin and the fused images, respectively. The proposed algorithm's flow chart is shown in Fig. (3). The input image's structure can be described using the entropy (E), a numerical value that represents a statistical measure of randomness [11]:

$$E = - \sum (f(I, j) \log_2 f(i, j)) \quad (10)$$

The histogram of an image is represented as f(I,j). Entropy typically employs 256 bins for 8-bit data and 2 bins for logically arranged arrays.

5. Results and Discussions

Fig. 4(a, b) shows the proposed algorithm on an MRI and CT images, respectively. The maximal fusion of the generated image is shown in figure 4(c).

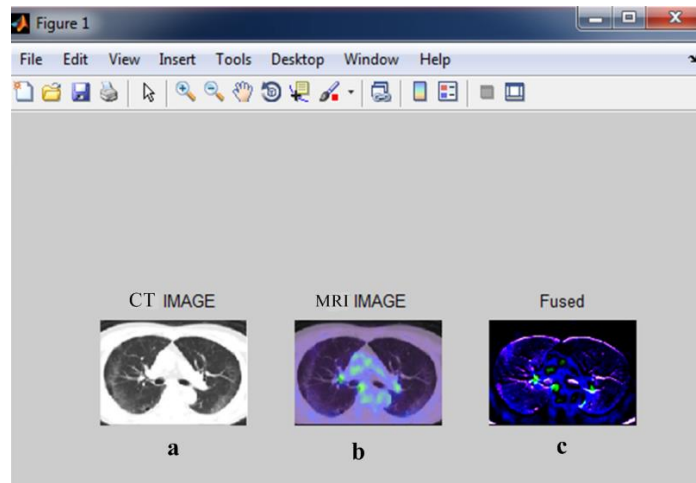


Figure 5. Input Images and Fusion Result. As a result, when compared to a and b, the infected parts are clearly visible in (c).

Table (1) presents the results of image integration using two plane waves, and the resulting image properties are measured by PSNR and entropy. The COVID-19 areas are detected.

Table 1. Performance appraisal of the fused image

WAVELETS	bior2.2	coif2	db2	dmey	rbio2.2	sym4	haar
PSNR	11.0579	11.1392	11.1664	11.1325	10.8037	11.1184	11.195
Entropy	8.3675	8.3206	8.4723	8.5245	8.3582	8.4069	8.3012

Figure (6) depicts the PSNR ratio of the data obtained from various wavelets, including bior2.2, coif2, db2, dmey, rbio2.2, sym4, and haar, we got the highest PSNR value when applying haar waves and its value was 11.195, it was the lowest. The PSNR value when applying the rbio2.2 waves was 11.0579.

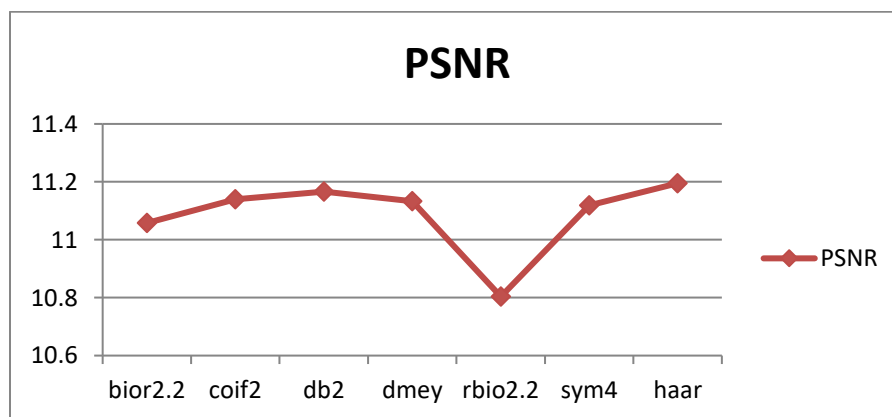


Figure 6. PSNR changes by using various wavelets at the second decomposition level.

Figure (7) displays the entropy values that were found with the corresponding values from the various wavelets being bior2.2, coif2, db2, dmey, rbio2.2, sym4, and haar. Entropy is achieved above the first level of decomposition, and it is clearly observed that the dmey waveforms reached a peak of 8.5245.

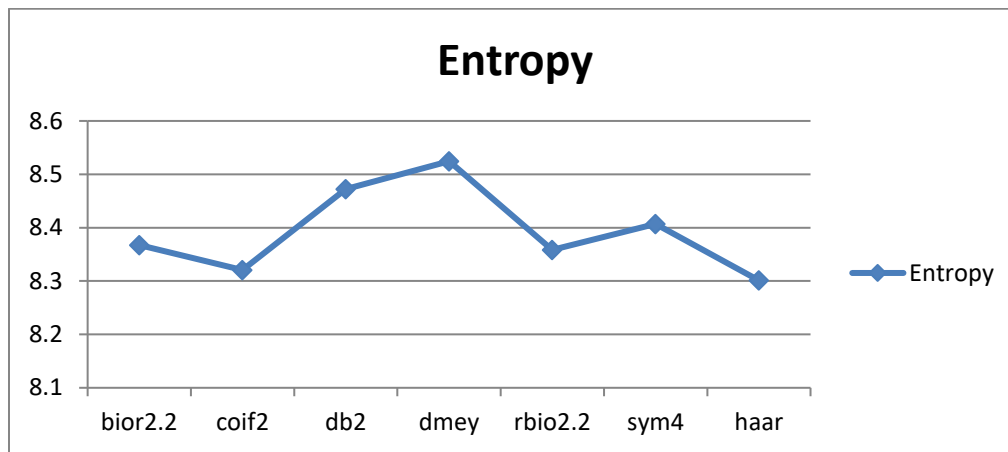


Figure 7. Entropy varies when several wavelets are used at the second decomposition level.

6. Conclusion

The Corona pandemic has devastated health systems in many countries, so it was necessary to detect the Corona virus (COVID-19) in a quick, easy and cheap way that could help reduce this disease and reduce the burden on the health system. A technique for merging multifocal images for the identification of COVID-19 to produce a significant image with multispectral data is based on wavelet transduction from computer tomography (CT) and magnetic resonance imaging (MRI) images. It automatically recognizes lung injuries and also identifies their exact position and intensity. The results of the array of images using various wavelengths were compared to the original MRI and CT images to determine lung injury based on PSNR and Entropy. It was found that although dmey waves performed best with entropy, haar waves performed best with PSNR. It was discovered that haar waves performed best with PSNR while dmey waves performed best with entropy. The results of the proposed method were accurate and fast Detection of coronavirus (COVID-19) in the lung

References

- [1] S. Udomhunsakul, and P. Wongsita, "Feature extraction in medical MRI images," *Proceeding of 2004 IEEE Conference on Cybernetics and Intelligent Systems*, vol. 1. p.p. 340- 344. 2004.
- [2] B. B. Hazarika, and D. Gupta "Modelling and forecasting of COVID-19 spread using wavelet-coupled random vector functional link networks", *Applied Soft Computing*, vol. 96, p. 106626, 2020.
- [3] M. Pahar, M. Klopper, R. Warren, and T. Niesler, "COVID-19 detection in cough, breath and speech using deep transfer learning and bottleneck features", *Computers in biology and medicine*, vol. 141, p. 105153, 2022.
- [4] V. Despotovic, M. Ismael, M. Cornil, R. Mc Call, & G. Fagherazzi, "Detection of COVID-19 from voice, cough and breathing patterns: Dataset and preliminary results", *Computers in Biology and Medicine*, vol. 138, p. 104944, 2021.
- [5] Y. E. Erdoğan, & A. Narin, "COVID-19 detection with traditional and deep features on cough acoustic signals", *Computers in Biology and Medicine*, vol. 136, p. 104765, 2021.
- [6] A. Sarhan. "Run length encoding based wavelet features for COVID-19 detection in X-rays". *BJR/ Open*, vol. 3. No. 1. p. 20200028, 2021.

- [7] K. Parmar, K. K. Rahul, and N. T. Falgun, "Analysis of CT and MRI on image fusion using wavelet transform." 2012 International Conference Communication Systems and Network Technologies. IEEE 2012.
- [8] S. Mane, and S. D. Sawant, "Image Fusion On Mr And Ct Images Using Wavelet Transforms And Dsp Processor." *International Journal of Engineering Trends and Technology (IJETT)*, vol. 4, 2013.
- [9] C. Y. N. Dwith, V. Angoth and A. Singh, "Wavelet based image fusion for detection of brain tumor", *International Journal of Image, Graphics and Signal Processing*, vol. 5, no. 1, p.p. 25, 2013.
- [11] I. Powell, M. J. D. "An algorithm for maximizing entropy subject to simple bounds", *Mathematical Programming*, vol. 42, no. (1), p.p. 171-180, 1988.
- [10] R. J. Sapkal, and S. M. Kulkarni, "Image fusion based on wavelet transform for medical application", *International Journal of Engineering Research and Applications*, vol.2.5, p.p. 624-627, 2012.